

The **next generation** GBCA
from Guerbet is here

Explore new possibilities >

Guerbet | 

© Guerbet 2024 GUOB220151-A

AJNR

This information is current as
of March 20, 2024.

Fast Contrast-Enhanced 4D MRA and 4D Flow MRI Using Constrained Reconstruction (HYPRFlow): Potential Applications for Brain Arteriovenous Malformations

W. Chang, Y. Wu, K. Johnson, M. Loecher, O. Wieben, M.
Edjlali, C. Oppenheim, P. Roca, J. Hald, B. Aagaard-Kienitz,
D. Niemann, C. Mistretta and P. Turski

AJNR Am J Neuroradiol 2015, 36 (6) 1049-1055

doi: <https://doi.org/10.3174/ajnr.A4245>

<http://www.ajnr.org/content/36/6/1049>

Fast Contrast-Enhanced 4D MRA and 4D Flow MRI Using Constrained Reconstruction (HYPRFlow): Potential Applications for Brain Arteriovenous Malformations

W. Chang, Y. Wu, K. Johnson, M. Loecher, O. Wieben, M. Edjlali, C. Oppenheim, P. Roca, J. Hald, B. Aagaard-Kienitz, D. Niemann, C. Mistretta, and P. Turski



ABSTRACT

BACKGROUND AND PURPOSE: HYPRFlow is a novel imaging strategy that provides fast, high-resolution contrast-enhanced time-resolved images and measurement of the velocity of the entire cerebrovascular system. Our hypothesis was that the images obtained with this strategy are of adequate diagnostic image quality to delineate the major components of AVMs.

MATERIALS AND METHODS: HYPRFlow and 3D TOF scans were obtained in 21 patients with AVMs with correlative DSA examinations in 14 patients. The examinations were scored for image quality and graded by using the Spetzler-Martin criteria. Mean arterial transit time and overlap integrals were calculated from the dynamic image data. Volume flow rates in normal arteries and AVM feeding arteries were measured from the phase contrast data.

RESULTS: HYPRFlow was equivalent to 3D-TOF in delineating normal arterial anatomy, arterial feeders, and nidus size and was concordant with DSA for AVM grading and venous drainage in 13 of the 14 examinations. Mean arterial transit time on the AVM side was 0.49 seconds, and on the normal contralateral side, 2.53 seconds with $P < .001$. Across all 21 subjects, the mean arterial volume flow rate in the M1 segment ipsilateral to the AVM was 4.07 ± 3.04 mL/s; on the contralateral M1 segment, it was 2.09 ± 0.64 mL/s. The mean volume flow rate in the largest feeding artery to the AVM was 3.86 ± 2.74 mL/s.

CONCLUSIONS: HYPRFlow provides an alternative approach to the MRA evaluation of AVMs, with the advantages of increased coverage, 0.75-second temporal resolution, 0.68-mm isotropic spatial resolution, and quantitative measurement of flow in 6 minutes.

ABBREVIATIONS: CE-VIPR = contrast-enhanced time-resolved vastly undersampled isotropic radial projection reconstruction; HYPR LR = highly constrained projection reconstruction using a local reconstruction convolution kernel; PC-VIPR = phase-contrast MRA using vastly undersampled isotropic radial projection reconstruction; HYPRFlow = highly constrained projection reconstruction using PC-VIPR flow images for the constraint

Many MR angiography techniques have been used for the imaging of arteriovenous malformations with various levels of efficacy. 3D-TOF imaging is capable of imaging arterial components of AVMs with high spatial resolution.^{1,2} However, it does not routinely visualize venous structures, which are important in

assessing AVMs, and does not acquire relevant hemodynamic information. 4D contrast-enhanced MRA has been reported to be of value for pre- and posttreatment assessment of AVMs by using Cartesian acquisitions, partial-Fourier encoding, and multicoil parallel imaging.³ However, because acquisition time increases proportionally with matrix size, obtaining an FOV and spatial resolution sufficient to visualize arteriovenous malformations can be challenging. Furthermore, low temporal resolution can also make delineation of small arterial feeders and venous drainage difficult with these techniques.³⁻⁹

Recent progress in constrained reconstruction techniques has suggested that it may be possible to overcome many of the limitations in temporal resolution, spatial resolution, and signal-to-noise ratio encountered by using conventional reconstruction schemes for time-resolved contrast-enhanced MRA. In such techniques, assumptions are made regarding the sparsity of images in time and space, and a priori information is used to guide or “constrain” the reconstruction. The assumptions are enforced during reconstruction using a nonlinear reconstruction. Unfortunately,

Received July 23, 2014; accepted after revision September 29.

From the Department of Radiology (W.C.), University of California, Los Angeles, Los Angeles, California; Departments of Radiology (B.A.-K., P.T.), Neurosurgery (D.N.), and Medical Physics (Y.W., K.J., M.L., O.W., C.M.), University of Wisconsin School of Medicine, Madison, Wisconsin; Department of Radiology (M.E., C.O., P.R.), Université Paris-Descartes, Paris, France; and Department of Radiology (J.H.), Rikshospitalet, Oslo, Norway.

This work was supported by the National Institutes of Health RO1NS066982.

Paper previously presented in part at: Annual Meeting of the American Society of Neuroradiology and the Foundation of the ASNR Symposium, April 21–26, 2012; New York, New York.

Please address correspondence to Patrick A. Turski, MD, University of Wisconsin Hospital, Radiology MC 3252, 600 Highland Ave, Madison, WI 53792; e-mail: pturski@uwhealth.org

Indicates open access to non-subscribers at www.ajnr.org

<http://dx.doi.org/10.3174/ajnr.A4245>

the utility of many such techniques has been limited by long reconstruction times due to the iterative nature of the reconstruction process.^{10,11}

In this work, we investigated the utility of a noniterative constrained acquisition and reconstruction scheme, HYPRFlow (highly constrained projection reconstruction using PC-VIPR flow images for the constraint), for the assessment of AVMs. The basis of HYPRFlow is that temporal resolution and spatial resolution are separated into 2 scans, a dynamic contrast-enhanced examination and a highly accelerated 3D phase-contrast angiogram. The 3D phase-contrast scan not only serves as a high-quality constraining image for the dynamic contrast-enhanced images but also provides velocity maps of the entire cerebrovascular system. While it is not presently realized clinically, this detailed flow information has the potential to improve characterization of AVMs and to assess treatment efficacy.^{12,13}

MATERIALS AND METHODS

Volunteer patient studies were performed in compliance with the Health Insurance Portability and Accountability Act regulations and by using a protocol approved by the local institutional review board. Subjects were recruited from patients undergoing clinical assessment for known brain arteriovenous malformations. Twenty-one adult subjects (14 women, 7 men) ranging from 27 to 69 years of age were imaged by using a 3T MR imaging system (Discovery 750; GE Healthcare, Milwaukee, Wisconsin) with an 8-channel head coil (HD Brain Coil; GE Healthcare).

Methods: Acquisition Strategy

A key element of HYPRFlow is the use of undersampled 3D radial trajectories to speed the acquisition (3D radial readout = vastly undersampled isotropic projection reconstruction [VIPR]). Radial imaging eliminates the time-consuming phase-encoding used in Cartesian acquisitions. Acceptable radial images can be generated from substantially fewer readouts than conventional Cartesian encoding, providing whole-brain imaging in a fraction of the imaging time. However, as the number of radial trajectories decreases, undersampling artifacts become apparent in the images. The undersampling artifacts can be removed or dramatically reduced by the constraining process.

Dynamic Scan. Fast serial 3D radial scans are obtained of the entire brain during the passage of a contrast agent by using only a small number of readouts. This dynamic acquisition is termed CE-VIPR (contrast-enhanced time resolved vastly undersampled isotropic radial projection reconstruction). Very fast temporal resolution can be achieved providing a whole-head 3D acquisition every 0.5 seconds.

Static Scan. High-resolution phase-contrast vastly undersampled radial projection reconstruction (PC-VIPR) angiograms and velocity measurements are acquired by using a 5-point flow-encoding strategy that increases the velocity-to-noise ratio.¹⁴ The phase-contrast angiograms are well-suited for highly constrained projection and local reconstruction (HYPR LR) because the stationary background tissue is subtracted out and the remaining vascular structures are sparse in the imaging volume.

Methods: Constrained Image Reconstruction Using HYPR LR

The reconstruction of HYPRFlow images by using HYPR LR¹⁵ can be formulated as follows:

$$I_H(t) = I_w^* \times I_C = \frac{I_t \times K}{I_C \times K} \times I_C,$$

where I_t is a reconstructed timeframe image from the dynamic scan, I_C is the phase-contrast constraint (PC-VIPR), and K is a $10 \times 10 \times 10$ (pixels) convolution kernel. To compensate for the signal variations due to the high undersampling, we applied a tornado-shaped filter with 0.5 seconds at the center of a k -space and 0.75 seconds at the cutoff frequency of the local kernel being applied. The result is a time-series of high-spatial-resolution MR angiographic images (voxel size, 0.68 mm^3) with the contrast kinetic features of high temporal resolution (0.75 seconds). The PC-VIPR velocity data can also be used for flow analysis. The entire acquisition is obtained in a clinically acceptable imaging time of 6 minutes. Reconstruction time for the HYPRFlow images ranged from 30 to 45 minutes. The strategy of combining rapid contrast-enhanced serial 3D radial imaging (CE-VIPR), phase-contrast radial imaging (PC-VIPR), and highly constrained projection reconstruction (HYPR LR) is termed “HYPRFlow” (Fig 1).¹²

By including both a dynamic series for the display of contrast kinetics and a phase-contrast acquisition to measure flow features, we anticipated that this strategy would be useful for the evaluation of high-flow conditions such as brain arteriovenous malformations. Our primary hypothesis is that the images obtained with this novel strategy are of adequate diagnostic quality to delineate the major components of AVMs.

HYPRFlow Imaging Protocol

Imaging parameters for the dynamic contrast-enhanced multi-echo 3D radial scan (CE-VIPR) were the following: FOV = $22 \times 22 \times 22 \text{ cm}^3$, TR/TE = 3.0/0.4 ms, bandwidth = 125 kHz, 64 points from the center to the edge of the k -space for each projection, frame rate = 0.5 seconds, spatial resolution = $1.7 \times 1.7 \times 1.7 \text{ mm}$. Gadobenate dimeglumine (MultiHance; Bracco Diagnostics, Princeton, New Jersey) was injected at 3 mL/s, and the contrast dose was 0.1 mL/kg followed by a 20-mL saline flush.

After the dynamic acquisition, a high-resolution 3D radial phase-contrast (PC-VIPR) examination is performed. The phase-contrast scan, in principle, could be acquired in any trajectory. However, to achieve high-spatial-resolution and whole-brain coverage within a reasonable scan time, a 3D radial trajectory is used to speed the phase-contrast acquisition.^{14,16,17}

Scanning parameters for postcontrast PC-VIPR were the following: FOV = 22 cm^3 , TR/TE = 8.1/2.8 ms, velocity encoding = 80 cm/s, bandwidth = 62.5 kHz. The readout matrix was 320 points per projection, and the spatial resolution for the phase-contrast study was 0.68 mm^3 . Seven thousand radial projections were acquired within approximately 5 minutes. For comparison of spatial resolution, 3D TOF examinations were obtained by using 4–5 overlapping slabs (TR/TE = 25/2.5 ms, FOV = 24 cm, Cartesian encoding, zero-filling, voxel size = 0.5-mm isotropic).

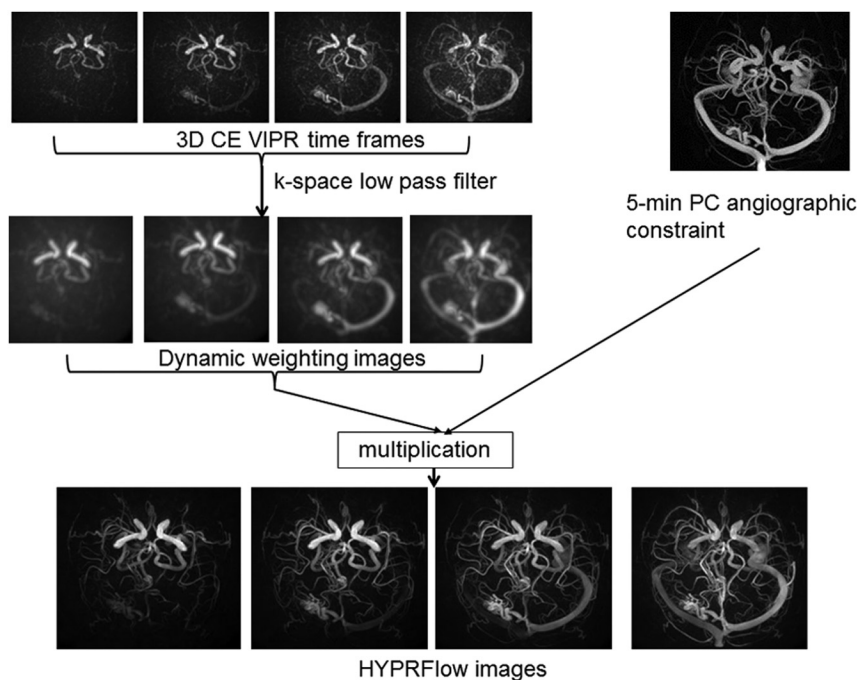


FIG 1. HYPRFlow image reconstruction. Top row: 60 whole-brain 3D radial scans are obtained every 0.5 seconds and reconstructed by using a 0.75-second acquisition window during the first passage of the contrast bolus. Four scans are displayed from this time-series (3D CE-VIPR time-frames). Top right: following the dynamic scan, a 3D radial phase-contrast MRA is obtained (5-minute PC-VIPR MRA used as the vascular constraint). Middle row: temporal weighting images are produced by using a low-pass filter. Bottom row: HYPR LR multiplication and reconstruction are performed by using the phase-contrast angiographic data to constrain the dynamic weighting images. Four HYPRFlow images from the 60-image time-series are displayed, demonstrating improved SNR and spatial resolution following HYPR LR reconstruction.

3D-TOF was included to allow comparison of the arterial anatomy with the highest resolution MRA method commercially available. The DSA studies were obtained within 8 weeks of the HYPRFlow scans by using an Artis zee biplane system (Siemens, Erlangen, Germany) with multiple projections, supplemented by 3D imaging and microcatheter-selective injections using imaging frame rates of 4–8 frames per second. DSA was considered the criterion standard for analysis.

Image Quality and Anatomic Analysis

HYPRFlow arterial and venous phase images and TOF images and DSA arterial and venous phase images were scored by 2 experienced neuroradiologists (with >25 years in practice) for image quality in the M2/M3 branches for all 3 modalities. Deep and superficial venous image quality was also scored for HYPRFlow and DSA.

The examinations were presented by using a clinical PACS workstation. Source and MIP images were reviewed. The MR imaging research coordinator randomized the examinations, attended each review session, and entered the data into the score sheet. Images were scored from 1–4 (scale: 1, poor visualization; 2, visualized but not of diagnostic quality; 3, good visualization of diagnostic quality; 4, excellent visualization and of excellent diagnostic quality). The largest diameter of the nidus was measured for all 3 modalities. In addition to scoring the venous image quality, the venous drainage pattern of each AVM was recorded as

superficial, deep, or mixed. The AVMs were graded by using the Spetzler-Martin scoring system.¹⁸

Flow Analysis

Quantitative measurement of the separation of arteries and veins for the time-resolved contrast-enhanced HYPRFlow images was assessed by generating contrast time curves obtained from the proximal middle cerebral artery and the vein of Trolard (or an analogous large cortical vein) ipsilateral and contralateral to the AVM. The overlap integral was calculated as the area of the overlapped region between arterial and venous contrast kinetic curves. The description of this approach for the evaluation of time-resolved contrast-enhanced MRA has been previously reported.^{19,20} A smaller overlap integral implies better arterial and venous separation. The overlap integrals were compared by using a 2-sample *t* test. In addition, mean arterial transit time was measured in the middle cerebral artery and the vein of Trolard (contralateral to the AVM) and the main feeding artery trunk (A1, M1, P1) and the earliest filling cortical vein (ipsilateral to the AVM).

The flow analysis of the PC-VIPR velocity data was performed by using a commercial software program (EnSight; CEI, Apex, North Carolina). Volume flow rates were measured in the proximal middle cerebral artery (ipsilateral and contralateral to the AVM) and the largest arterial feeder to the AVM.

Statistical Analysis

Image quality values for HYPRFlow were compared with both TOF and DSA. TOF was also directly compared with DSA by using the Wilcoxon rank sum test. A *P* value < .05 was considered a significant difference between modalities. Maximum nidus diameter was measured for all 3 modalities, and the Wilcoxon rank sum test was used to compare the results.

RESULTS

Anatomic Analysis

When we compared M2/M3 arterial branches, there was no significant difference between the mean image quality scores of HYPRFlow (3.18) and TOF (3.26) (*P* > .05), but there were very significant differences between the image quality of both HYPRFlow and TOF compared with DSA (3.94) with *P* < .002 and .004, respectively. DSA deep and superficial venous image quality (3.82) was significantly better than HYPRFlow (3.08) (*P* < .005) (Figs 2–4).

Differences in the maximum diameter of the nidus were not significant between HYPRFlow (mean diameter, 32.4 mm) and DSA (mean diameter, 34.3 mm) (Wilcoxon rank sum test, *P* = .11). How-

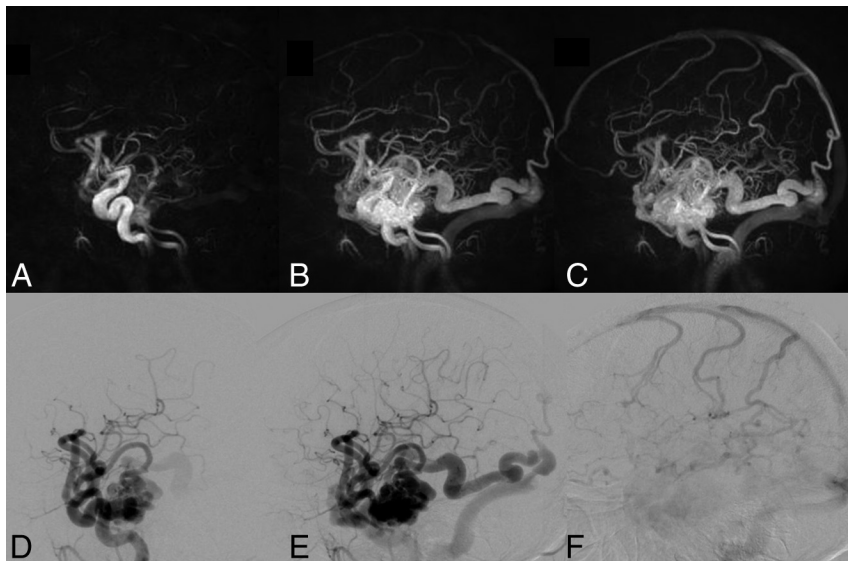


FIG 2. Right temporal lobe AVM. Top row: 3 HYPRFlow images from the 60-image dynamic series. Arterial (A), mixed (B), and venous phase (C) images are displayed. Bottom row: corresponding DSA arterial (D), mixed (E), and venous phase (F) images. The HYPRFlow images demonstrate the cortical venous drainage similar to the DSA.

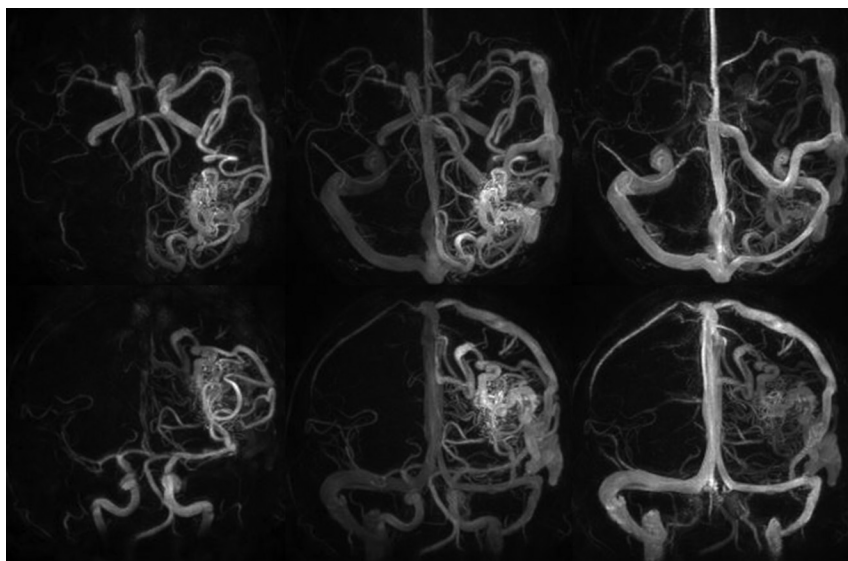


FIG 3. HYPRFlow images of a left parietal occipital AVM, demonstrating whole-brain coverage and isotropic 0.68-mm resolution. Top row: axial HYPRFlow MIP images left to right: arterial, mixed, and venous phase. Bottom row: the same image data projected into the coronal plane, left to right: arterial, mixed, and venous phase images.

ever, there was a statistically significant difference ($P = .016$) when TOF (mean diameter, 30.2 mm) was compared with DSA.

The Spetzler-Martin grades and number of patients in each category based on DSA were grade I ($n = 2$), grade II ($n = 4$), grade III ($n = 3$), grade IV ($n = 3$), and grade V ($n = 2$) (Figs 2–4). There was 1 instance in which very small deep medullary draining veins were not identified on the HYPRFlow examination, resulting in disagreement with the DSA Spetzler-Martin grade (Fig 5); otherwise HYPRFlow and DSA were in concordance.

Flow Analysis

A 2-sample t test revealed a significant difference between the mean arterial transit time on the AVM side (0.49 seconds) com-

pared with the normal contralateral side (2.53 seconds) with $P < .001$. A 2-sample t test revealed a significant difference between the overlap integral of the AVM (0.92) compared with the normal side (0.82) with $P < .001$. The mean arterial volume flow rate in the M1 ipsilateral to the AVM across all subjects was 4.07 ± 3.04 mL/s, the contralateral mean arterial volume flow rate was 2.09 ± 0.64 mL/s, and the mean volume flow rate measured in the largest feeding artery to the AVM was 3.86 ± 2.74 mL/s.

DISCUSSION

Evaluation of cerebral arteriovenous malformations is challenging with existing MRA methods because AVMs can be extensive, requiring a large FOV but also containing very small features that require high spatial resolution. The rapid flow and arteriovenous shunting intrinsic to AVMs demands high temporal resolution. The criterion standard for the evaluation of arteriovenous malformations is digital subtraction angiography, which has extremely high temporal and spatial resolution. However, DSA provides limited physiologic information, exposes patients to ionizing radiation, uses iodinated contrast agents carrying a risk of renal injury or allergic reaction, and is an invasive procedure with a risk of iatrogenic stroke.²¹ 4D CT angiography is another technique that has high spatial and temporal resolution, accurately delineates the vascular components of AVMs, but also exposes patients to iodinated contrast agents and ionizing radiation.²² The advantages of combining MR imaging and MRA have led to continued interest in the use of MR angiography in the study of AVMs. Although time-resolved contrast-enhanced MRA using Cartesian phase en-

coding has a wide safety margin, the risk of nephrogenic systemic fibrosis must be considered in patients with renal failure.²³ TOF MRA has spatial resolution approaching that of CT angiography, displays arterial elements with excellent image quality, and has clinically acceptable acquisition times.²⁴ However, it does not routinely provide assessment of the venous drainage and dynamic information on vessel filling or arteriovenous shunts. Phase-contrast MRA (4D flow MR imaging) has been used to visualize AVMs, provide flow analysis of AVMs, and monitor treatment effects.^{13,25} Multiple studies have demonstrated that Cartesian-based 4D time-resolved contrast-enhanced MRA using Cartesian phase encoding can characterize the major components of AVMs.

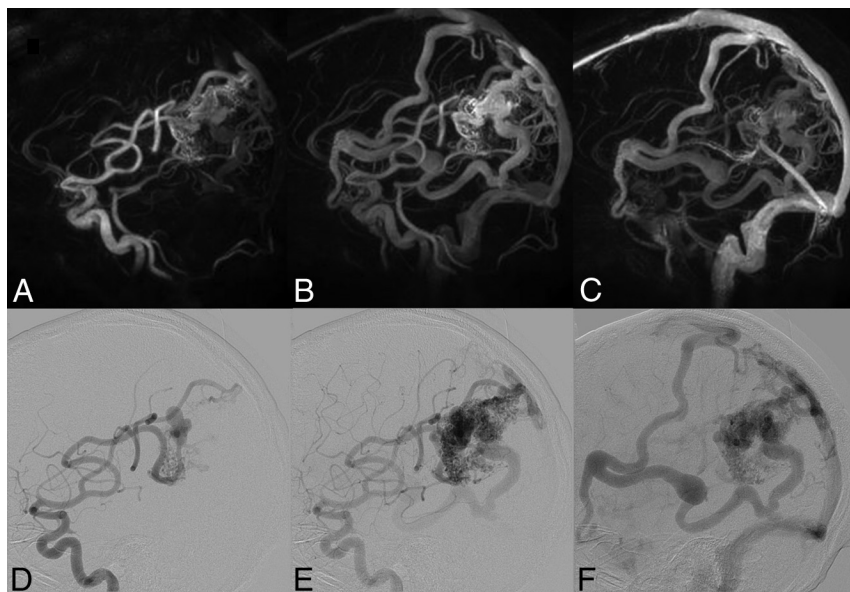


FIG 4. The same patient as shown in Fig 3. Top row: HYPRFlow images in the sagittal plane: arterial (A), mixed (B), and venous phase (C). Bottom row: corresponding DSA images: arterial (D), mixed (E), and venous phase (F). Note the excellent correlation of the arterial supply and venous drainage pattern.

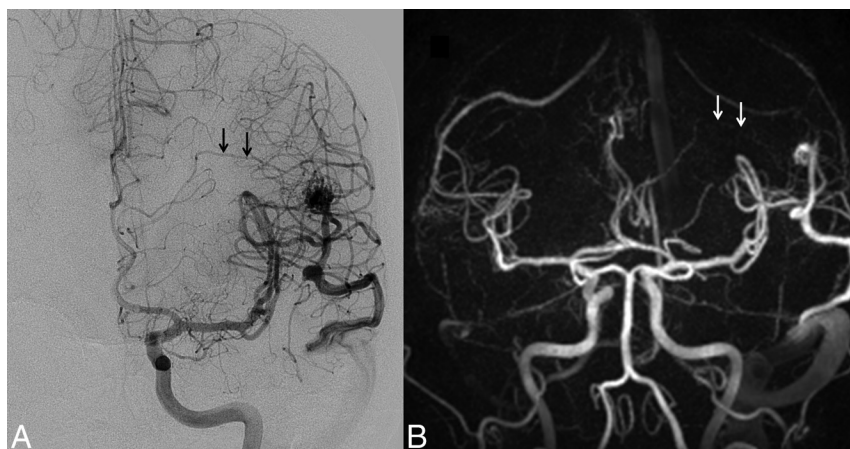


FIG 5. Left posterior frontal AVM. A, The DSA examination demonstrates a small deep medullary vein (arrows), which drains into the straight sinus. The AVM nidus was in close proximity to the Broca area and was scored as Spetzler-Martin grade III. B, Coronal HYPRFlow late arterial phase image with poor delineation of the deep medullary vein (arrows), resulting in incorrect classification of the AVM as Spetzler-Martin grade II.

Current Cartesian encoding methods use variable k -space sampling, parallel imaging, and temporal correlations to accelerate the acquisition and improve resolution, but these methods are typically limited in coverage.^{3,4,7-9,26} Noncontrast 4D arterial spin-labeling methods provide excellent temporal resolution and arterial imaging; venous imaging with these methods can be limited due to transit-time signal decay.²⁷⁻²⁹ Radial encoding without constrained reconstruction has been successfully used to accelerate acquisition and imaging of AVMs but has SNR limitations.³⁰ The advantage of combining radial encoding and constrained reconstructions to increase SNR has been previously demonstrated in healthy subjects³¹ and patients with AVMs.³²

HYPRFlow is a highly innovative approach that overcomes many of the limitations of previous methods. Whole-brain

coverage for both the dynamic CE-VIPR and static PC-VIPR scans allows a global assessment of the entire cerebrovascular system, enabling characterization of the AVM and alterations in flow in adjacent vascular territories. HYPRFlow is well-suited to study AVMs because in addition to the global anatomic coverage, the dynamic series can be used to measure contrast kinetics such as contrast arrival time, time to peak, overlap integral, and transit time. Our results show that transit time can be quantitated and that it is dramatically shortened compared with the contralateral analogous vessels. We further estimated the magnitude of the arteriovenous shunting by measuring the overlap integral for the largest artery supplying the AVM and compared this value with the analogous contralateral vessels. The analysis of contrast kinetics is augmented by the addition of flow encoding of the entire cerebrovascular system. Our flow analysis results demonstrate that flow measurements can be easily accomplished in primary arterial segments (A1, M1, and P1 segments) and major arterial branches supplying the AVM. Although we performed a limited flow analysis for this report, the HYPRFlow velocity data can be used to generate flow path lines,¹³ estimate wall shear stress,³³ measure pulsatility, quantitate velocity/flow,²⁵ and identify pressure gradients.³⁴

One of the appealing features of HYPRFlow is the ability to image both the venous drainage of the AVM and the global venous drainage of the entire cerebrovascular system. The dynamic contrast-enhanced images provide detailed anatomic depiction of the venous drainage and have adequate resolution to identify venous stenosis and varices.

The anatomic images can then be used to guide the flow analysis by using the PC-VIPR velocity data. For example, with the velocity data, venous outflow can be quantified and pressure gradients can be measured across regions of venous outflow obstruction. Risk stratification for patients with AVMs remains a challenge, and continued investigation of both anatomic features and hemodynamics is warranted because there are few well-established criteria to identify high-risk populations.³⁵⁻³⁷

Limitations

While this study demonstrates that HYPRFlow is well-suited to assess AVMs, there are still multiple challenges. Patient motion may result in misregistration of the dynamic and static scans, resulting in image blurring after constrained reconstruction. Un-

dersampling artifacts may also be a concern; however, the artifacts are limited by the sparsity of neurovascular structures in the imaging volume and the location of the artifacts predominantly outside the ROI. The sample size of patients is small, limiting generalization of the findings. The flow analysis was limited to major arterial structures, and no hemodynamic measurements were made of the venous components. There may also be vascular signal loss in the PC-VIPR data due to spin-dephasing from complex flow. The impact of hemosiderin and other blood products on the image quality of the HYPRFlow images was not systematically reviewed. However, signal loss due to blood products would fall under the general class of artifacts related to susceptibility phase dispersion and subsequent signal loss. Susceptibility-based signal loss was a major aspect of our analysis. The short TE of the PC-VIPR sequence reduces but does not eliminate signal loss due to susceptibility effects.

Another limitation is the challenge related to detecting aneurysms within and remote from the nidus. Previous reports have shown that aneurysms can be accurately identified when a portion of the signal from the contrast-enhanced magnitude dataset (the contrast-enhanced 3D radial T1-weighted component of the phase-contrast acquisition) is combined with the flow images.³⁸ However, this approach was not used in this investigation due to the large size of the datasets and the lack of automated processing tools. Consequently, systematic analysis of aneurysm detection was not performed. The velocity dependence of PC-VIPR may result in loss of signal in very slow-flow structures, though this is reduced by the use of contrast enhancement and 5-point flow encoding and can be overcome by including a component of the magnitude data in the reconstruction.³⁸ Finally, reconstruction by using HYPRFlow takes 30–45 minutes and requires noncommercial software.

CONCLUSIONS

This study demonstrates that HYPRFlow compares favorably with 3D-TOF for the evaluation of arterial feeders and AVM nidus size. There was no significant difference in the measurement of the maximum diameter of the nidus between HYPRFlow and DSA, and there was only 1 discrepancy in assessing venous drainage. HYPRFlow provides a more comprehensive evaluation of AVMs, delineating the arterial supply, nidus size, and venous drainage and offers contrast kinetics and hemodynamic information.

Disclosures: Kevin Johnson—*RELATED: Grant:* National Institutes of Health*; *UNRELATED: Patents (planned, pending or issued):* US patent pending. *Comments:* Contrast-Enhanced MRA with Highly Constrained Backprojection Reconstruction Using Phase Contrast Composite Image, US Patent No. 7991452. Under our agreements, I may be entitled to a portion of the licensing fees if this technology were put into a commercial product; *Royalties:* US Patent Royalties; *Other:* research support from GE Healthcare.* Pauline Roca—*RELATED: Grant:* GE Healthcare.* *Comments:* I had a postdoctoral position funded by GE Healthcare from June 1, 2011, to May 31, 2013. Beverly Aagaard-Kienitz—*RELATED: Grant:* GE Healthcare.* *Comments:* GE Healthcare provides support to the University of Wisconsin MR imaging research program. The investigators do not receive any direct funding. Charles Mistretta—*RELATED: Grant:* National Institutes of Health*; *Support for Travel to Meetings for the Study or Other Purposes:* National Institutes of Health*; *UNRELATED: Grants/Grants Pending:* National Institutes of Health, *Comments:* 4D DSA and 4D fluoroscopy; *Payment for Lectures (including service on Speakers Bureaus):* various universities, *Comments:* typical visiting professor lectures; *Patents (planned, pending or issued):* I have several recent patents related to x-ray work; *Royalties:* Wisconsin Alumni

Research Foundation. *Comments:* royalties on several MR imaging patents. Patrick Turski—*RELATED: Grant:* National Institutes of Health RO1 NS066982.* *Comments:* National Institutes of Health RO1 NS066982 provides support for development of accelerated MRA techniques; *UNRELATED: Other:* GE Healthcare.* *Comments:* GE Healthcare provides support to the University of Wisconsin MR imaging research program. The investigators do not receive any direct funding.* Money paid to the institution.

REFERENCES

- Heidenreich JO, Schilling AM, Unterharnscheidt F, et al. **Assessment of 3D-TOF-MRA at 3.0 Tesla in the characterization of the angioarchitecture of cerebral arteriovenous malformations: a preliminary study.** *Acta Radiol* 2007;48:678–86
- Loy DN, Rich KM, Simpson J, et al. **Time-of-flight magnetic resonance angiography imaging of a residual arteriovenous malformation nidus after Onyx embolization for stereotactic radiosurgery planning: technical note.** *Neurosurg Focus* 2009;26:E13
- Hadizadeh DR, Kukuk GM, Steck DT, et al. **Noninvasive evaluation of cerebral arteriovenous malformations by 4D-MRA for preoperative planning and postoperative follow-up in 56 patients: comparison with DSA and intraoperative findings.** *AJNR Am J Neuroradiol* 2012;33:1095–101
- Gauvrit JY, Leclerc X, Oppenheim C, et al. **Three-dimensional dynamic MR digital subtraction angiography using sensitivity encoding for the evaluation of intracranial arteriovenous malformations: a preliminary study.** *AJNR Am J Neuroradiol* 2005;26:1525–31
- Gauvrit JY, Oppenheim C, Nataf F, et al. **Three-dimensional dynamic magnetic resonance angiography for the evaluation of radiosurgically treated cerebral arteriovenous malformations.** *Eur Radiol* 2006;16:583–91
- Hadizadeh DR, von Falkenhausen M, Gieseke J, et al. **Cerebral arteriovenous malformation: Spetzler-Martin classification at subsecond-temporal-resolution four-dimensional MR angiography compared with that at DSA.** *Radiology* 2008;246:205–13
- Taschner CA, Gieseke J, Le Thuc V, et al. **Intracranial arteriovenous malformation: time-resolved contrast-enhanced MR angiography with combination of parallel imaging, keyhole acquisition, and k-space sampling techniques at 1.5 T.** *Radiology* 2008;246:871–79
- Petkova M, Gauvrit JY, Trystram D, et al. **Three-dimensional dynamic time-resolved contrast-enhanced MRA using parallel imaging and a variable rate k-space sampling strategy in intracranial arteriovenous malformations.** *J Magn Reson Imaging* 2009;29:7–12
- Oleaga L, Dalal SS, Weigele JB, et al. **The role of time-resolved 3D contrast-enhanced MR angiography in the assessment and grading of cerebral arteriovenous malformations.** *Eur J Radiol* 2010;74:e117–21
- Mistretta CA. **Undersampled radial MR acquisition and highly constrained back projection (HYPR) reconstruction: potential medical imaging applications in the post-Nyquist era.** *J Magn Reson Imaging* 2009;29:501–16
- Wu Y, Chang W, Johnson KM, et al. **Fast whole-brain 4D contrast-enhanced MR angiography with velocity encoding using undersampled radial acquisition and highly constrained projection reconstruction: image-quality assessment in volunteer subjects.** *AJNR Am J Neuroradiol* 2011;32:E47–50
- Velikina JV, Johnson KM, Wu Y, et al. **PC HYPR flow: a technique for rapid imaging of contrast dynamics.** *AJNR Am J Neuroradiol* 2010;31:447–56
- Ansari SA, Schnell S, Carroll T, et al. **Intracranial 4D flow MRI: toward individualized assessment of arteriovenous malformation hemodynamics and treatment-induced changes.** *AJNR Am J Neuroradiol* 2013;34:1922–28
- Johnson KM, Markl M. **Improved SNR in phase contrast velocimetry with five-point balanced flow encoding.** *Magn Reson Med* 2010;63:349–55
- Johnson KM, Velikina J, Wu Y, et al. **Improved waveform fidelity using local HYPR reconstruction (HYPR LR).** *Magn Reson Med* 2008;59:456–62

16. Gu T, Korosec FR, Block WF, et al. **PC VIPR: a high-speed 3D phase-contrast method for flow quantification and high-resolution angiography.** *AJNR Am J Neuroradiol* 2005;26:743–49
17. Johnson KM, Francois C, Lum D, et al. **Rapid comprehensive evaluation of luminography and hemodynamic function with 3D radially undersampled phase contrast imaging MRI.** *Conf Proc IEEE Eng Med Biol Soc* 2009;2009:4057–60
18. Spetzler RF, Martin NA. **A proposed grading system for arteriovenous malformations.** *J Neurosurg* 1986;65:476–83
19. Cashen TA, Jeong H, Shah MK, et al. **4D radial contrast-enhanced MR angiography with sliding subtraction.** *Magn Reson Med* 2007;58:962–72
20. Wu Y, Johnson K, Kecskemeti SR, et al. **Time resolved contrast enhanced intracranial MRA using a single dose delivered as sequential injections and highly constrained projection reconstruction (HYPR CE).** *Magn Reson Med* 2011;65:956–63
21. Willinsky RA, Taylor SM, TerBrugge K, et al. **Neurologic complications of cerebral angiography: prospective analysis of 2,899 procedures and review of the literature.** *Radiology* 2003;227:522–28
22. Wang H, Ye X, Gao X, et al. **The diagnosis of arteriovenous malformations by 4D-CTA: a clinical study.** *J Neuroradiol* 2014;41:117–23
23. Sadowski EA, Bennett LK, Chan MR, et al. **Nephrogenic systemic fibrosis: risk factors and incidence estimation.** *Radiology* 2007;243:148–57
24. Buis DR, Bot JC, Barkhof F, et al. **The predictive value of 3D time-of-flight MR angiography in assessment of brain arteriovenous malformation obliteration after radiosurgery.** *AJNR Am J Neuroradiol* 2012;33:232–38
25. Markl M, Wu C, Hurley MC, et al. **Cerebral arteriovenous malformation: complex 3D hemodynamics and 3D blood flow alterations during staged embolization.** *J Magn Reson Imaging* 2013;38:946–50
26. Willinek WA, Hadizadeh DR, von Falkenhausen M, et al. **4D time-resolved MR angiography with keyhole (4D-TRAK): more than 60 times accelerated MRA using a combination of CENTRA, keyhole, and SENSE at 3.0T.** *J Magn Reson Imaging* 2008;27:1455–60
27. Yu S, Yan L, Yao Y, et al. **Noncontrast dynamic MRA in intracranial arteriovenous malformation (AVM), comparison with time of flight (TOF) and digital subtraction angiography (DSA).** *Magn Reson Imaging* 2012;30:869–77
28. Raoult H, Bannier E, Maurel P, et al. **Hemodynamic quantification in brain arteriovenous malformations with time-resolved spin-labeled magnetic resonance angiography.** *Stroke* 2014;45:2461–64
29. Wu H, Block WF, Turski PA, et al. **Noncontrast dynamic 3D intracranial MR angiography using pseudo-continuous arterial spin labeling (PCASL) and accelerated 3D radial acquisition.** *J Magn Reson Imaging* 2014;39:1320–26
30. Eddleman CS, Jeong HJ, Hurley MC, et al. **4D radial acquisition contrast-enhanced MR angiography and intracranial arteriovenous malformations: quickly approaching digital subtraction angiography.** *Stroke* 2009;40:2749–53
31. Chang W, Landgraf B, Johnson KM, et al. **Velocity measurements in the middle cerebral arteries of healthy volunteers using 3D radial phase-contrast HYPRFlow: comparison with transcranial Doppler sonography and 2D phase-contrast MR imaging.** *AJNR Am J Neuroradiol* 2011;32:54–59
32. Jeong HJ, Cashen TA, Hurley MC, et al. **Radial sliding-window magnetic resonance angiography (MRA) with highly-constrained projection reconstruction (HYPR).** *Magn Reson Med* 2009;61:1103–13
33. Chang W, Loecher MW, Wu Y, et al. **Hemodynamic changes in patients with arteriovenous malformations assessed using high-resolution 3D radial phase-contrast MR angiography.** *AJNR Am J Neuroradiol* 2012;33:1565–72
34. Moftakhar R, Aagaard-Kienitz B, Johnson K, et al. **Noninvasive measurement of intra-aneurysmal pressure and flow pattern using phase contrast with vastly undersampled isotropic projection imaging.** *AJNR Am J Neuroradiol* 2007;28:1710–14
35. Stapf C, Mast H, Sciacca RR, et al. **Predictors of hemorrhage in patients with untreated brain arteriovenous malformation.** *Neurology* 2006;66:1350–55
36. Mohr JP, Kejda-Scharler J, Pile-Spellman J. **Diagnosis and treatment of arteriovenous malformations.** *Curr Neurol Neurosci Rep* 2013;13:324
37. van Beijnum J, van der Worp HB, Buis DR, et al. **Treatment of brain arteriovenous malformations: a systematic review and meta-analysis.** *JAMA* 2011;306:2011–19
38. Kecskemeti S, Johnson K, Wu Y, et al. **High resolution three-dimensional cine phase contrast MRI of small intracranial aneurysms using a stack of stars k-space trajectory.** *J Magn Reson Imaging* 2012;35:518–27